IEEE Access
Multidisciplinary | Rapid Review | Open Access Journal

Received July 22, 2019, accepted August 25, 2019, date of publication August 29, 2019, date of current version September 12, 2019.

Digital Object Identifier 10.1109/ACCESS.2019.2938222

Unbalance Compensation and Automatic Balance of Active Magnetic Bearing Rotor System by Using Iterative Learning Control

YANGBO ZHENG, NI MO, YAN ZHOU, AND ZHENGANG SHI

Institute of Nuclear and New Energy Technology, Tsinghua University, Beijing 100084, China
Collaborative Innovation Center of Advanced Nuclear Energy Technology, Tsinghua University, Beijing 100084, China
Key Laboratory of Advanced Reactor Engineering and Safety, Ministry of Education, Tsinghua University, Beijing 100084, China

Corresponding author: Zhengang Shi (shizg@tsinghua.edu.cn)

This work was supported by the National Science and Technology Major Project of China under Grant 2019ZX06903019.

ABSTRACT Active control is one of the most important advantages of active magnetic bearing (AMB), and also can be used to suppress the imbalance of AMB rotor system (AMB-RS). This paper aims at dealing with periodic vibration problem caused by unbalanced force existing in AMB-RS as the rotor spins. Firstly, with the advantages of iterative learning control (ILC) over repetitive problems, a novel ILC algorithm based on the system information of the iteration before last iteration is put forward to achieve parallel computing of real-time control, real-time acquisition and signal extraction in AMB digital control system (DCS). Then, two compound control modes are proposed on the basis of AMB closed-loop feedback control system (CFCS), one is a parallel compound control mode (PCCM) that is used to achieve unbalance compensation, the other one is a serial compound control mode (SCCM) that is used to achieve automatic balance, and corresponding compound control systems are designed on the basis of an AMB experimental system. Finally, numerical simulation and experimental research are carried out, and the results show that the control methods proposed in this paper have significant control effect on the periodic vibrations produced by the unbalanced force of AMB-RS. Therefore, the research achievements can provide theoretical references and experimental basis for the further application of AMB in the high-precision and high-speed fields.

INDEX TERMS Active magnetic bearing rotor system (AMB-RS), iterative learning control (ILC), parallel compound control mode (PCCM), serial compound control mode (SCCM), unbalance compensation, automatic balance.

I. INTRODUCTION

AMB, as a preferred rotor support technology for high-precision, high-speed and high-cleaning fields, has advantages of no mechanical friction, no lubrication, low loss, etc. More importantly, active control provides the technical foundation for the unbalanced force detection and control of AMB-RS, and also provides active vibration control means for mechanical device equipped with AMB [1]. For example, AMB is put forward to suppress the unbalanced magnetic pull produced by the motor in [2], and the application of AMB in vibration control is discussed and analyzed in detail in [3].

The vibrations produced by unbalanced force on the rotor have periodic repetitive characteristics with same frequency or multi-frequency of the rotating speed in rotational machines equipped with AMB. Such as rotor mass imbalance and sensor runout [4], [5], which are the main sources of the synchronous vibrations, geometric misalignment between stator and rotor of the motor [6] and asymmetric electrical parameters in magnetic poles of the AMB and the motor [7], [8], which are the main sources of the multi-frequency vibrations. Fortunately, the active control function of AMB can be used to suppress the rotor vibrations. However, due to open-loop instability of the AMB-RS, a closed-loop feedback controller (FC) is usually used to achieve the stability control of the system, but the FC is not ideal in suppressing periodic vibrations of the rotor, so other control methods are always introduced to suppress the vibrations.

In [8]–[10], the unbalance control methods of AMB-RS are usually divided into two categories: unbalance compensation and automatic balance. Among them, unbalance

The associate editor coordinating the review of this article and approving it for publication was Wojciech Paszke.

compensation is to offset the existing unbalanced force by the opposite force generated in controller, to ensure the rotor spins the geometric axis, which is also known as force-control mode and suitable for high-precision fields, such as [11]–[13]. Similarly, automatic balance is to achieve rotor spins freely around its inertial axis by ignoring the periodic component of rotor vibration signal in the control process, which is also known as force-freedom mode and suitable for high-speed fields, such as [7], [14], [15].

Among these unbalance control methods, some algorithms rely heavily on the rotor system model, and most algorithms are only studied in theory and simulation, but not fully verified in the actual AMB system. As we know, AMB-RS is a typical multi-input multi-output (MIMO), strongly coupled and nonlinear system. More seriously, there also exists certain uncertainties of the system model during operation. Therefore, it is difficult to apply the unbalance control methods which rely on the system model to actual AMB system. In recent years, some researchers have introduced ILC into unbalance control of AMB-RS, and some research results are achieved in [13], [16]. However, some details are not elaborated in depth, and they belong to unbalance compensation control methods. Moreover, automatic balance control method achieved by ILC is little proposed, and its experimental research is never mentioned before.

But in fact, ILC has been widely and successfully applied in other fields with repetitive control requirements. In the past two decades, lots of researches have been performed in the theory and application of ILC, such as [17]–[27]. From these research results, ILC has unique advantages in dealing with repetitive problems as it adopts a learning mechanism by using previous system information. Moreover, it has been successfully applied in robot repetitive operation control, high-precision motion control, motor disturbance suppress, industrial process control and so on.

To sum up, this paper fully combines the technical advantages of ILC with the requirements of periodic vibration suppression of the AMB-RS, and presents a novel ILC algorithm and two compound control strategies for unbalance control of AMB-RS, then designs corresponding control systems for unbalance compensation and automatic balance, to meet the requirements of different applications.

And this paper is arranged as follows: Section II presents the control plant of AMB and points out the problems of the periodic vibrations generated by unbalanced force. In Section III, a novel ILC algorithm and two compound control strategies for unbalance control of AMB-RS are proposed and analyzed in detail. In Section IV, numerical simulation and experiment research are carried out to verify the effectiveness of the methods, and the results are discussed in detail. Finally, some conclusions and future works are summarized in Section V.

II. PROBLEM FORMULATION

From the current application status, only those rotational mechanical equipment operating in special fields would be equipped with AMB system, such as high-speed motors, energy storage flywheels, primary helium circulators and so on. In one of our projects [28], the clearance between rotor and auxiliary bearing is only 0.15mm. Obviously, if the amplitude of vibration produced by unbalanced force on the rotor exceeds the maximum permissible range, collision would be occurred. In mild cases, the collision may lead to deterioration of the equipment operation performance, but in severe cases, the collision may lead to the serious damage of the rotational mechanical equipment or system. Therefore, the safe and reliable control of rotor system determine the development and application of AMB technology. In practical applications, the stability control of AMB system is usually achieved by FCs, which are always implemented based on PID algorithm. In order to keep the consistency with the AMB experimental system adopted later in this paper, a single degree-of-freedom (DOF) radial model of vertical AMB is taken as an example to describe the problem.

A. THE CONTROL PLANT OF AMB WITH A SINGLE DOF

In an AMB system, a pair of identical electromagnets installed in the direction of 180° are usually used to achieve the differential drive mode and the stability control in one direction is shown in Fig.1. Here, the differential drive mode refers to that the actual current flowing through the electromagnet is composed of bias current i_{x0} and control current i_{xc}. Therefore, the actual excitation currents flowing through two symmetric electromagnets can be expressed as:

$$\begin{cases} i_1 = i_{x0} + i_{xc} \\ i_2 = i_{x0} - i_{xc} \end{cases} \tag{1}$$

where i_{x0} is a constant current that is set according to the AMB structure and system operation requirements, and i_{xc} is a real-time control current that is changed according to the rotor operation condition. These combination described as equation (1) can ensure that the AMB is operating stably near the equilibrium point.

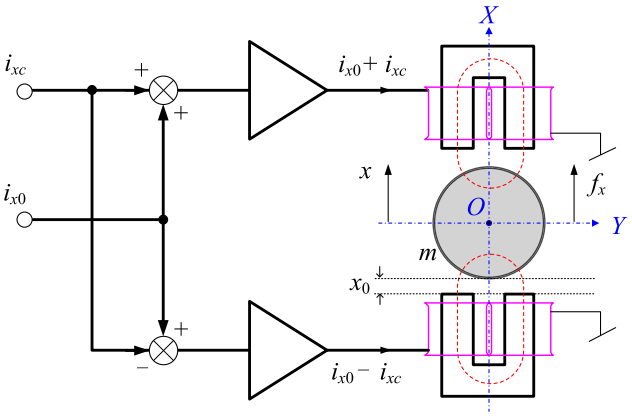

FIGURE 1. Differential drive mode of AMB.

According to Maxwell's electromagnetic theory and the equivalent theory of magnetic circuit, the electromagnetic

force generated by a single electromagnet is:

$$f = k\frac{i^2}{\tilde{x}^2} \tag{2}$$

where i is the actual current flowing through the electromagnet, $\tilde{x}$ is the air gap length between the rotor and magnetic pole, and k is the electromagnetic force coefficient. Certainly, k is a constant for a given AMB system and is calculated by equation (3).

$$k = \frac{1}{4}\mu_0 N_0^2 A_0 \tag{3}$$

where μ_0 is the permeability of vacuum, N_0 is the coil turns of electromagnet, and A_0 is the effective magnetic pole area. When the differential drive mode shown in Fig. 1 is adopted, the electromagnetic force of AMB-RS in one direction (X direction is taken as an example) can be expressed as:

$$f_x = f_{X+} - f_{X-} = k[\frac{(i_{x0}+i_{xc})^2}{(x_0-x)^2} - \frac{(i_{x0}-i_{xc})^2}{(x_0+x)^2}] \tag{4}$$

where, x_0 is the air gap length when the rotor operates at the equilibrium point, and x is the rotor displacement. Here, Taylor linearization is always carried out at the equilibrium point (i_{x0}, x_0), then we can get

$$f_x \approx f_x(i_{x0}, x_0) + \frac{\partial f_x}{\partial x}|_{(i_{x0},x_0)}(x - x_0) + \frac{\partial f_x}{\partial i_c}|_{(i_{x0},x_0)}(i_{xc} - i_{x0}) \tag{5}$$

Equation (5) can be simplified to

$$f_x = k_{xi} i_{xc} + k_x x \tag{6}$$

where, k_{xi} is the force-current coefficient and k_x is the force-displacement coefficient. They are two constants for a given AMB system, and calculated by equations (7).

$$\begin{cases} k_{xi} = \dfrac{\mu_0 A_0 N^2 i_0}{x_0^2} \\ k_x = \dfrac{\mu_0 A_0 N^2 i_0^2}{x_0^3} \end{cases} \tag{7}$$

According to Newton's second law, we can get

$$m\ddot{x} = k_{xi} i_{xc} + k_x x \tag{8}$$

where m is the rotor mass. By using the Laplace transform technique, the transfer function of the AMB with a single DOF can be described as

$$G_{sAMB}(s) = \frac{k_{xi}}{ms^2 - k_x} \tag{9}$$

Equation (9) indicates that the AMB with a single DOF is an open-loop unstable system. So a CFCS shown in Fig. 2 is used to meet stability control requirements.

In Fig.2, K_{PA} and K_{DS} are the power amplifier coefficient and displacement sensor coefficient respectively, and they are also two constants for a given AMB system.

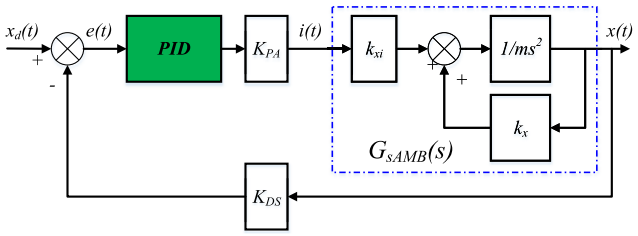

FIGURE 2. The CFCS of AMB with a single DOF.

B. PERIODIC VIBRATIONS GENERATED BY UNBALANCED FORCE

From the above analysis, it seems that the stability control of AMB is not difficult. But actually, the force on AMB-RS is very complex, as it includes periodic and non-periodic components. This paper mainly studies the suppression of periodic vibrations caused by unbalanced force because they are the main components of the vibrations and the most dangerous to the system. In order to more clearly illustrate the periodic vibrations of the rotor system, a schematic diagram of the end face structure of AMB is shown in Fig.3.

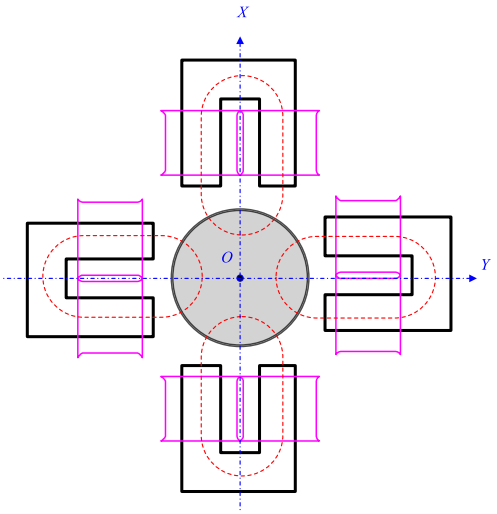

FIGURE 3. The schematic diagram of the end face structure of AMB.

Here we assume that the electromagnetic forces are f_x and f_y and unbalanced forces are f_{xd} and f_{yd} in the radial X and Y directions respectively. Then according to Newton's second law,

$$\begin{cases} m\ddot{x} = f_x + f_{xd} \\ m\ddot{y} = f_y + f_{yd} \end{cases} \tag{10}$$

According to equation (6), we can get

$$\begin{cases} f_x = k_{xi} i_{xc} + k_x x \\ f_y = k_{yi} i_{yc} + k_y y \end{cases} \tag{11}$$

In an AMB system, electromagnets are usually configured in pairs and with several magnetic poles. Typically, four pairs of electromagnets with eight poles are the most commonly

used in AMB system as shown in Fig.3. Further, according to the research results of [12], [29], [30], the main component of the periodic vibrations are low frequency periodic vibrations, especially, synchronous vibration is the most serious. This is the reason that most of unbalance control methods only consider the suppression synchronous vibration. So, here we only discuss and analyze the constant component, the first component and the second component of unbalanced forces.

$$\begin{cases} f_{xd} = \sum_{n=0}^{2} c_{xn} \sin(n\omega t + \varphi_{xn}) \\ f_{yd} = \sum_{n=0}^{2} c_{yn} \cos(n\omega t + \varphi_{yn}) \end{cases}, \quad n\epsilon\{0, 1, 2\} \qquad (12)$$

where c_{xn} and c_{yn} are the amplitudes of unbalanced forces, φ_{xn} and φ_{yn} are the phases of unbalanced forces, ω is the rotating speed and t is the time. In addition, $n = 0$ represents the constant component, $n = 1$ represents the first component and $n = 2$ represents the second component.

Ideally, when AMB-RS operates at the equilibrium point, the resultant force on the rotor should be zero and the rotor only rotates under the drive of the motor. However, the actual AMB-RS is subject to the unbalanced force shown in equation (12). Specially, according to the closed-loop feedback control principle of AMB shown in Fig.2, the FC can generate the corresponding force to balance the unbalanced forces. Importantly, the FC should completely balance the constant component ($n = 0$) of the unbalanced forces, which is the prerequisite for stable operation of AMB system. Unfortunately, the FC is continuously trying to generate forces to compensate for the first and second components of periodic unbalanced forces ($n = 1, 2$). But according to Newton's third law of action and reaction principle, when the magnetic poles generate electromagnetic forces that act on the rotor, the magnetic poles would also be subject to reaction forces, which lead to periodic vibrations of the AMB system. In more detail, the nonlinear vibration equations produced by the rotor under the periodic unbalanced force can be expressed as:

$$\begin{cases} m\ddot{x} + c\dot{x} + k_0 x = \sum_{n=1}^{2} c_{xn} \sin(n\omega t + \varphi_{xn}) \\ m\ddot{y} + c\dot{y} + k_0 y = \sum_{n=1}^{2} c_{yn} \cos(n\omega t + \varphi_{yn}) \end{cases} \qquad (13)$$

where c is rotor damping and k_0 is rotor stiffness. The vibration equations described as equations (13) are based on the rigid characteristics of AMB-RS in the experimental system, if it is a flexible rotor, the vibration equations would be more complex.

From the form of solution to equations (13), the displacement components of the rotor are consistent with the unbalanced force components in the X and Y directions. In other words, the rotor moves in the form of simple harmonic vibration, which means that there exists the synchronous vibration and double-frequency vibration. Obviously, the compound motion of the rotor in two directions would be a round, oval, heart-shaped, petal-shaped or other more complex loci, which are determined by the amplitude and phase of simple harmonic vibration in two directions. However, these periodic vibrations cannot be suppressed effectively by FC, so they are the difficult control issues of AMB system.

But in the high-precision or high-speed fields, the vibration amplitude of the rotor must be suppressed within a reasonable and feasible level as much as possible, and the rotor must operate at a deterministic geometric position. For example, in high-temperature gas-cooled reactor project, the vibration amplitude of the rotor in the primary helium circulator should be suppressed within $4.5 \times 10^{-5} m$.

III. CONTROL METHOD

From the above analysis, it can be seen that the periodic vibrations of AMB-RS caused by the unbalanced forces have the relation with the same frequency and multi-frequency of the rotating speed, which lay a foundation for introducing the ILC to suppress the unbalanced forces. However, one requirement of ILC is that the system needs to be completely reset to the initial state after each iteration. Fortunately, the asynchronous iterative learning mechanism proposed in [17] lays a theoretical foundation for the unbalance control application of AMB-RS. As asynchronous ILC is used in the rotor unbalance control, the time (T) of one rotation is used as the iterative learning period, and the phase of the speed detected by real-time speed sensor is used to trigger each iteration. Therefore, asynchronous ILC algorithm applicable to unbalanced control of AMB-RS can be described as:

$$\begin{aligned} u_{(k+1)T}(t) = \mathcal{F}(&u_0(t), u_T(t), \cdots, u_{kT}(t), \\ &e_0(t), e_T(t), \cdots, e_{kT}(t), e_{(k+1)T}(t)) \end{aligned} \qquad (14)$$

where T is the time of one rotation, k is the iterative number.

A. A NOVEL ITERATIVE LEARING MECHANISM

In the AMB system, vibrations are not only caused by certain unbalanced factors, but also caused by a large number of random factors. That is, the real-time displacement information collected by the displacement sensor contains non-periodic components. Coupled with the interference of environmental noise, the displacement information finally collected may not have significant periodic repetitive characteristics. Therefore, most of the unbalance control algorithms of AMB-RS need to extract periodic component from the displacement information. That is to say, the control system needs to filter the displacement information of each rotation, which is the basis of most current control methods for rotor unbalance of AMB-RS. Similarly, this process is important for ILC in unbalance control of AMB-RS. Notably, due to ILC only has a significant control effect on repetitive problems, non-repetitive problems would worsen the control performance.

The periodic component extraction of displacement information mentioned here is usually based on Fourier transform theory. In this paper, the process of the synchronous vibration extraction is taken as an example for principle analysis [10], [12], [30]. And the corresponding extraction algorithms are shown in equations (15)-(18), and the process

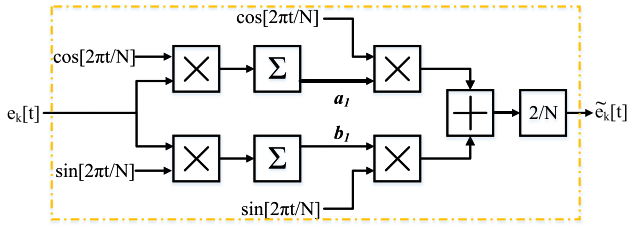

FIGURE 4. The synchronous vibration extraction principle of AMB-RS.

is shown in Fig.4.

$$\begin{cases} a_1 = \sum_{i=0}^{N-1} e_k[i] \cos(\frac{2\pi i}{N}) \\ b_1 = \sum_{i=0}^{N-1} e_k[i] \sin(\frac{2\pi i}{N}) \end{cases} \tag{15}$$

$$\tilde{e_k}[i]|_{i=0}^{N-1} = \frac{2}{N}\left(a_1 \cos\left(\frac{2\pi i}{N}\right) + b_1 \sin\left(\frac{2\pi i}{N}\right)\right) \tag{16}$$

$$\tilde{e_k}[i]|_{i=0}^{N-1} = A_1 \cos(\frac{2\pi i}{N} - \theta) \tag{17}$$

$$\begin{cases} A_1 = \frac{2}{N}\sqrt{a_1^2 + b_1^2} \\ tan\theta = \frac{b_1}{a_1} \end{cases} \tag{18}$$

where, $e_k[i]|_{i=0}^{N-1}$ is the sequence of control errors in the *kth* iteration, the result of extraction is $\tilde{e}_k[i]|_{i=0}^{N-1}$, which has the sinusoidal periodic characteristic. N is the length of control error sequence, and it has

$$N = T/T_f \tag{19}$$

where, T_f is the sampling period of AMB control system. Obviously, the extraction described above is a non-causal data filtering method, and can only be carried out while a complete error sequence is obtained after each rotation.

Furthermore, we know that the discrete Fourier transform and its inverse transform require a lot of computational resources. Although only a few low-frequency components or only the same frequency component are needed to be analyzed in the unbalanced control of AMB-RS, the length of the control error sequence is usually very long. For example, if the rotor operates at 2,400 rpm ($f = 40$ Hz) and $T_f = 1 \times 10^{-4}s$, then we can get $N = 250$ as equation (19). In this case, the control system needs to call the sine or cosine function 1000 times. However, in DSP embedded systems, calling library functions like these complex operations would take up a lot of computing resources [31]. In the initial stage of our study, it was found that the packet loss rate was more than 20% as this problem was not considered. Finally, the results of this problem is that the real-time performance of ILC loop cannot be guaranteed well.

In order to solve the above problems, a novel parallel iterative control mechanism by using the system information of the iteration before last iteration is proposed here. So asynchronous ILC algorithm applicable to unbalanced control of AMB-RS can be rewritten as:

$$u_{(k+1)T}(t) = \mathcal{F}(u_{(k-1)T}(t), \tilde{e}_{(k-1)T}(t)) \tag{20}$$

Through this ingenious design of the algorithm, the control system can achieve the parallel processing of three processes: ILC, real-time displacement signal acquisition and periodic component extraction, which can ensure the control system has enough time to complete the analysis and calculation of the control error. The principle of these three parallel processes is shown in Fig.5.

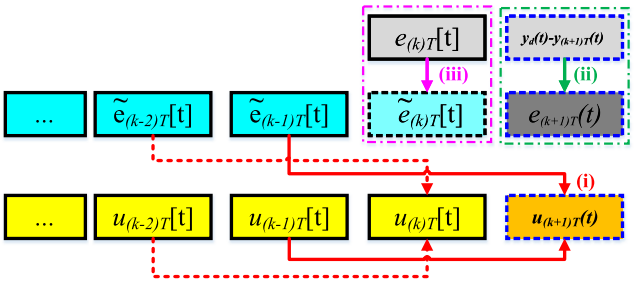

FIGURE 5. The novel parallel ILC mechanism by using the system information of the iteration before last iteration.

The three parallel processes described in Fig.5 are expressed as

$$\begin{cases} u_{(k+1)T}(t) = \mathcal{F}\left(u_{(k-1)T}(t), \tilde{e}_{(k-1)T}(t)\right) & (i) \\ e_{(k+1)T}(t) = y_d(t) - y_{(k+1)T}(t) & (ii) \\ e_{(k)T}[t] \rightarrow \tilde{e}_{(k)T}[t] & (iii) \end{cases} \tag{21}$$

where, $y_d(t)$ is the target displacement of the rotor, and $y_{(k+1)T}(t)$ is the real-time displacement of the $(k+1)$th iteration. In more detail, when the rotation ends, that is, the (k)th iteration ends, a complete control error sequence $e_{(k)T}[t]$ is collected by the control system. $\tilde{e}_{(k)T}[t]$ does not exist because extraction algorithms have not been executed, but meanwhile the $(k+1)$th iteration is performed immediately. Therefore, in the novel ILC mechanism, the control input of the $(k+1)$th ILC is generated by using the $(k-1)$th system information($u_{(k-1)T}(t)$ *and* $\tilde{e}_{(k-1)T}(t)$). At the same time, displacement information $e_{(k+1)T}(t)$ is acquired in real time for FC and ILC, and $\tilde{e}_{(k)T}[t]$ is extracted from $e_{(k)T}[t]$ for the $(k+2)$th iteration.

B. THE NOVEL ILC FOR UNBANLCE CONTROL OF AMB-RS

There are two advantages of this novel ILC, one is the repetitive control advantage of ILC can effectively suppress the periodic vibrations, the other one is the parallel processing mechanism can ensure the real-time performance of ILC loop. Obviously, this ingenious algorithm mechanism is simple and convenient to implement, especially it can ensure real-time performance of the ILC loop.

But the convergence rate of control error is slower than that of ILC based on the system information of the last iteration. Our previous simulation research results show that, the iterations of the novel ILC is twice as much as the iterations

of the ILC based on system information of the last iteration with the same initial error, final error, algorithm structure and parameters. But it is perfectly acceptable in the unbalance control of AMB-RS. Further, considering the rigid characteristics of AMB-RS in the experimental system, an open-loop differential type ILC with a variable forgetting factor and a variable learning gain is adopted here, as expressed in equation (22).

$$\begin{aligned} u_{(k+1)T}(t) = &\left(1-\xi_{ff}(k-1)\right)u_{(k-1)T}(t) \\ &+\xi_{ff}(k-1)\,u_0(t)+\mathcal{L}_{(k-1)T} \\ &(k-1,t)(\tilde{e}_{(k-1)T}(t+1)-\tilde{e}_{(k-1)T}(t)) \end{aligned} \quad (22)$$

where $u_0(t)$ is the initial control, the variable forgetting factor is $\xi_{ff}(k-1)$ that is changed with iterations, and the variable learning gain is $\mathcal{L}_{(k-1)T}(k-1,t)$ that is changed with iterations and time step.

Here, the AMB rotor system with single degree of freedom (DOF) is taken as an example to analyze the convergence of the algorithm. The model of the system can be described as:

$$\begin{cases} \boldsymbol{x}_{(k)T}(t+1) = \boldsymbol{A}(t)\boldsymbol{x}_{(k)T}(t)+\boldsymbol{B}(t)u_{(k)T}(t) \\ y_{(k)T}(t) = \boldsymbol{C}(t)\boldsymbol{x}_{(k)T}(t) \end{cases} \quad (23)$$

where $u_{(k)T}(t) \in R$, $y_{(k)T}(t) \in R$ and $\boldsymbol{x}_{(k)T}(t) \in R^n$ are the input, output and state matrixes, and the system control objective is expressed as

$$\lim_{k\to\infty} e_{(k)T}(t) = \lim_{k\to\infty}\left[y_d(t)-y_{(k)T}(t)\right] = 0 \quad (24)$$

Now we assume that there exists a unique target control input sequence $u_d(t)$ for the target output sequence$y_d(t)$. Thus the goal of ILC is to find the target control input sequence $u_d(t)$ through iterations until $y_{(k)T}(t)$ track $y_d(t)$.

The solution of the state equation of the discrete system expressed in equation (23) is described as

$$\boldsymbol{x}_{(k)T}(t) = \boldsymbol{\Phi}(t,0)\,\boldsymbol{x}_{(k)T}(0)+\sum_{l=0}^{t-1}\boldsymbol{\Phi}(t,l+1)\,\boldsymbol{B}(l)\,u_{(k)T}(l), \quad (0\le t\le T) \quad (25)$$

where $\boldsymbol{x}_{(k)T}(0)$ is the initial states of the system.

Here,we analyze the convergence of the algorithm by using the periodic component of the system control error. The analysis process is described as follows:

$$\begin{aligned} &\tilde{e}_{(k+1)T}(t+1) \\ &= y_d(t+1)-y_{(k+1)T}(t+1) \\ &= y_d(t+1)-y_{(k-1)T}(t+1) \\ &\quad -\left(y_{(k+1)T}(t+1)-y_{(k-1)T}(t+1)\right) \\ &= \tilde{e}_{(k-1)T}(t+1)-\boldsymbol{C}(t+1) \\ &\quad \times\left(\boldsymbol{x}_{(k+1)T}(t+1)-\boldsymbol{x}_{(k-1)T}(t+1)\right)=\tilde{e}_{(k-1)T}(t+1) \\ &\quad -\sum_{l=0}^{t}\boldsymbol{C}(t+1)\,\boldsymbol{\Phi}(t+1,l+1)\,\boldsymbol{B}(l)\,u_{(k+1)T}(l) \\ &\quad +\sum_{l=0}^{t}\boldsymbol{C}(t+1)\,\boldsymbol{\Phi}(t+1,l+1)\,\boldsymbol{B}(l)\,u_{(k-1)T}(l) \end{aligned} \quad (26)$$

where $\tilde{e}_{(k+1)T}(t+1) = y_d(t+1)-y_{(k+1)T}(t+1)$ is an approximate representation because the method proposed in this paper only conducts the periodic component of the system control error. And now equation (22) is substituted into equation (26), it can be get

$$\begin{aligned} &\tilde{e}_{(k+1)T}(t+1) \\ &= \tilde{e}_{(k-1)T}(t+1)-\xi_{ff}(k-1) \\ &\quad \times\left(\sum_{l=0}^{t}\mathbf{C}(t+1)\,\boldsymbol{\Phi}(t+1,l+1)\,\boldsymbol{B}(l)\,(u_0(t+1)\right. \\ &\quad \left.-u_{(k+1)T}(l))\right) \\ &\quad -\boldsymbol{C}(t+1)\,\boldsymbol{B}(l)\,\mathcal{L}_{(k-1)T}(k-1,t) \\ &\quad \times\tilde{e}_{(k-1)T}(t+1)-\sum_{l=0}^{t-1}\boldsymbol{C}(t+1)\,\boldsymbol{\Phi}(t+1,l+1) \\ &\quad \times\boldsymbol{B}(l)\,\mathcal{L}_{(k-1)T}(k-1,t)\,\tilde{e}_{(k-1)T}(t+1) \\ &\quad +\sum_{l=0}^{t}\boldsymbol{C}(t+1) \\ &\quad \times\boldsymbol{\Phi}(t+1,l+1)\,\boldsymbol{B}(l)\,\mathcal{L}_{(k-1)T}(k-1,t)\,\tilde{e}_{(k-1)T}(t) \\ &= \left(1-\xi_{ff}(k-1)-\mathbf{C}(t+1)\,\boldsymbol{B}(l)\,\mathcal{L}_{(k-1)T}(k-1,t)\right) \\ &\quad \times\tilde{e}_{(k-1)T}(t+1)-\sum_{l=0}^{t-1}\mathbf{C}(t+1)\,\boldsymbol{\Phi}(t+1,l+1) \\ &\quad \times\boldsymbol{B}(l)\,\mathcal{L}_{(k-1)T}(k-1,t)\,\tilde{e}_{(k-1)T}(t+1) \\ &\quad +\sum_{l=0}^{t}\boldsymbol{C}(t+1) \\ &\quad \times\boldsymbol{\Phi}(t+1,l+1)\,\boldsymbol{B}(l)\,\mathcal{L}_{(k-1)T}(k-1,t)\,\tilde{e}_{(k-1)T}(t) \end{aligned} \quad (27)$$

The norm of both sides of equation (27) satisfies the relation expressed in equation (28).

$$\begin{aligned} &\left\|\tilde{e}_{(k+1)T}(t+1)\right\| \\ &\le \left\|1-\xi_{ff}(k-1)-\boldsymbol{C}(t+1)\right. \\ &\quad \left.\times\boldsymbol{B}(l)\,\mathcal{L}_{(k-1)T}(k-1,t)\right\|\left\|\tilde{e}_{(k-1)T}(t+1)\right\| \\ &\quad +\sum_{l=0}^{t-1}\|\boldsymbol{C}(t+1) \\ &\quad \times\boldsymbol{\Phi}(t+1,l+1)\,\boldsymbol{B}(l)\,\mathcal{L}_{(k-1)T}(k-1,t)\| \\ &\quad \times\left\|\tilde{e}_{(k-1)T}(t+1)\right\| \\ &\quad +\sum_{l=0}^{t}\|\boldsymbol{C}(t+1) \\ &\quad \times\boldsymbol{\Phi}(t+1,l+1)\,\boldsymbol{B}(l)\,\mathcal{L}_{(k-1)T}(k-2,t)\| \\ &\quad \times\left\|\tilde{e}_{(k-1)T}(t)\right\| \le \rho\left\|\tilde{e}_{(k-1)T}(t+1)\right\|+2a_1 \\ &\quad \times\sum_{l=0}^{t-1}\left\|e_{(k-1)T}(l+1)\right\|, (0\le t\le T) \end{aligned} \quad (28)$$

where, we define

$$\begin{cases} \rho = \left\|1-\xi_{ff}(k-1)-\boldsymbol{C}(t+1)\right. \\ \qquad \left.\boldsymbol{B}(t)\,\mathcal{L}_{(k-1)T}(k-1,t)\right\| \\ a_1 = \sup\limits_{0\le t\le T,0\le l\le t}\|\boldsymbol{C}(t+1)\,\boldsymbol{\Phi}(t,l+1) \\ \qquad \boldsymbol{B}(l)\,\mathcal{L}_{(k-1)T}(k-1,t)\| \end{cases} \quad (29)$$

Multiply both sides of equation (28) by λ^t $(0 < \lambda < 1)$, it can be get

$$\begin{aligned}
&\lambda^{t+1} \left\| \tilde{e}_{(k+1)T}(t+1) \right\| \\
&\quad \le \rho\lambda^{t+1} \left\| \tilde{e}_{(k-1)T}(t+1) \right\| \\
&\qquad + 2a_1 \sum_{l=0}^{t-1} \lambda^{t-l}\lambda^{l+1} \left\| e_{(k-1)T}(l+1) \right\| \\
&\quad \le \rho\lambda^{t+1} \left\| \tilde{e}_{(k-1)T}(t+1) \right\| \\
&\qquad + 2a_1 \sum_{l=0}^{t-1} \lambda^{t-l} \sup_{0\le l\le T} \{\lambda^{l+1} \left\| e_{(k-1)T}(l+1) \right\|\} \\
&\quad \le \rho\lambda^{t+1} \left\| \tilde{e}_{(k-1)T}(t+1) \right\| \\
&\qquad + 2a_1 \frac{\lambda(1-\lambda^T)}{1-\lambda} \sup_{0\le l\le T} \{\lambda^{l+1} \left\| e_{(k-1)T}(l+1) \right\|\} \quad (30)
\end{aligned}$$

The supremum of equation (30) can be written as

$$\sup_{0\le l\le T} \{\lambda^{t+1} \left\| \tilde{e}_{(k+1)T}(t+1) \right\| \le \tilde{\rho}\lambda^{l+1} \left\| e_{(k-1)T}(l+1) \right\|\}, \quad (0 \le t \le T) \quad (31)$$

where,

$$\tilde{\rho} = \rho + 2a_1 \frac{\lambda(1-\lambda^T)}{1-\lambda} \quad (32)$$

When the determined parameters are selected to meet $\rho < 1$, there must exists a λ to ensure $\tilde{\rho} < 1$, i.e.

$$\lim_{k\to\infty} \sup_{0\le l\le T} \{\lambda^{t+1} \left\| \tilde{e}_{(k+1)T}(t+1) \right\|\} = 0 \quad (33)$$

Since the process of the algorithm is to successively search the target input sequence $u_d(t)$, equation (22) can be rewritten as the parameters selected should meet the convergence requirement stated above.

$$\lim_{k\to\infty} u_{(k+1)T}(t) = \lim_{k\to\infty} u_{(k-1)T}(t) \quad (34)$$

To sum up, the convergence conditions for a single input single output (SISO) plant with the control algorithm expressed in equation (22) can be summarized as follows:

$$\begin{cases} |1 - \xi_{ff}(k) - \mathcal{L}(k,t)\boldsymbol{C}(t+1)\boldsymbol{B}(t)| < 1 \\ \lim\limits_{k\to\infty} \xi_{ff}(k) = 0 \end{cases} \quad (35)$$

Here, the initial control input and two variables can be set as equations (36), (37) and (38).

$$u_0(t) = 0 \quad (36)$$

$$\xi_{ff}(k) = \frac{1}{k} \quad (37)$$

$$\mathcal{L}_{(k)T}(k,t) = k_{BC}\frac{1}{k}e^{\frac{t}{N}} \quad (38)$$

Here, k_{BC} is a parameter determined by the convergence condition. Combining equations (22),(37) and (38), we know that

$$\lim_{k\to\infty} \left(1 - \xi_{ff}(k)\right) = 1 \quad (39)$$

$$\lim_{k\to\infty} k_{BC}\frac{1}{k}e^{\frac{t}{N}} = 0 \quad (40)$$

In other words, as $k \to \infty$, the control input of the systems meets

$$\lim_{k\to\infty} u_{(k+1)T}(t) = \lim_{k\to\infty} u_{(k-1)T}(t) = u_d(t) \quad (41)$$

where, $u_d(t)$ is the target control input. Equation (42) indicates that the target control input sequence can be got by performing ILC repeatedly. In other words, the control error would meet

$$\lim_{k\to\infty} e_k(t) = 0 \quad (42)$$

C. THE COMPOUND SCHEMES BASED ON THE NOVEL ILC

Obviously, the ILC expressed in equation (22) has no stability control effect on the system, that is, FC is necessary used to achieve the stability by CFCS and the ILC is used to suppress the periodic vibrations. Therefore, a compound scheme should be set to combine with FC and ILC to achieve control objectives. Certainly, there are various combinations of FC and ILC [33]–[35], and different combinations can be achieved according to different control objectives. Here, in order to achieve a plug-in control mechanism and simplicity design of a compound control system, this paper adopts a PCCM to achieve the unbalance compensation of AMB-RS and a SCCM to achieve the automatic balance of AMB-RS.

1) THE UNBALANCE COMPENSATION OF AMB-RS BASED ON THE NOVEL ILC

A PCCM of the FC and ILC is shown in Fig.6.

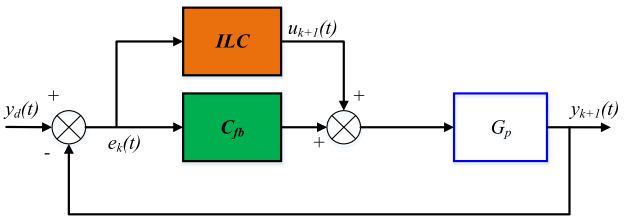

FIGURE 6. A PCCM of the FC and ILC.

In Fig.6, the ILC input and FC input are directly superimposed as the input of the controlled plant, so it is called PCCM, and the input and output relationship of this control system in frequency domain can be expressed as follows

$$\begin{aligned}
y_{k+1}(s) = &\left(1 + G_pC_{fb}\right)^{-1} G_pu_{k+1}(s) \\
&+ (1 + G_pC_{fb})^{-1} G_pC_{fb}y_d(s) \quad (43)
\end{aligned}$$

When this PCCM is used for unbalanced control of AMB-RS, the control signal generated by the ILC compensates the control signal generated by the FC to suppress periodic vibrations of the rotor. More directly, the real-time corrective control in FC and periodic compensation control in ILC are performed simultaneously, to achieve control objectives. So it is also called force-control method in the unbalanced control of AMB-RS as both controllers generate control signals of periodic vibrations.

In addition, in the perspective of the parallel control mechanism, there must exist control deviation as long as the rotor deviates from the equilibrium position (geometric axis), and the FC and ILC must generate corresponding signals to control the rotor spins the geometric axis. This means that the target balance position of the rotor is the geometric axis under the PCCM. So, we can see that this PCCM is suitable for the rotor unbalance control of AMB-RS in high-precision fields. And the PCCM realized finally in DCS is shown in Fig.7, in which the FC of the AMB is always a PID controller.

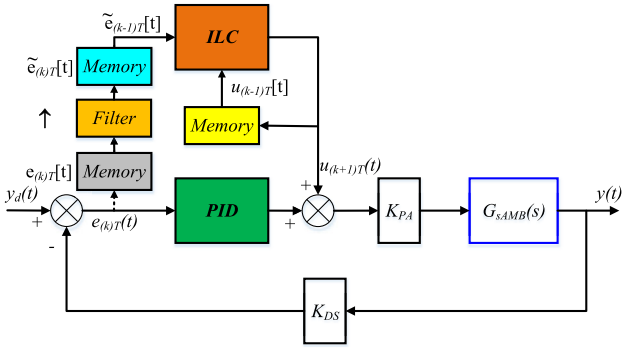

FIGURE 7. The PCCM achieved in DCS.

2) THE AUTOMATIC BALANCE OF AMB-RS BASED ON THE NOVEL ILC

A SCCM of the FC and ILC is shown in Fig.8.

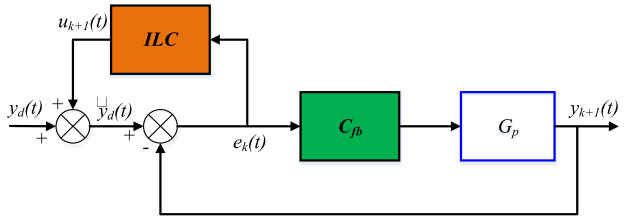

FIGURE 8. A SCCM of the FC and ILC.

In Fig.8, before entering the FC, $e_k\ (t)$ would be adjusted by the ILC to modify the reference input $y_d\ (t)$, which can compensate the $y_{k+1}\ (t)$. So it is a SCCM, and the input and output relationship of this control system in frequency domain can be expressed as follows:

$$y_{k+1}\ (s) = \left(1 + G_p C_{fb}\right)^{-1} G_p C_{fb} u_{k+1}\ (s) + (1 + G_p C_{fb})^{-1} G_p C_{fb} y_d\ (s) \quad (44)$$

When this SCCM is used for unbalanced control of AMB-RS, the ILC can generate the compensation signal with the same of frequency, phase and amplitude as the displacement signal, which can eliminate the effect of the FC on the periodic vibrations of the rotor. More directly, the FC is not aware of the periodic vibration under this SCCM, and the FC does not need to generate the compensation signal, so it is also called the force-freedom method.

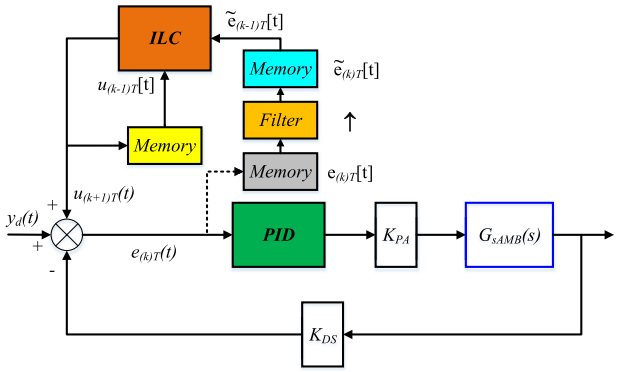

FIGURE 9. The SCCM achieved in DCS.

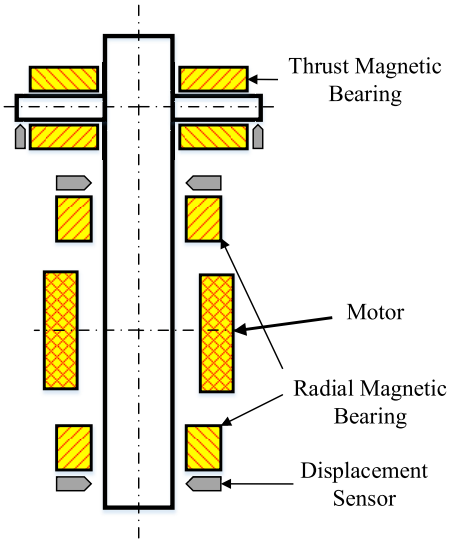

FIGURE 10. A vertical AMB structure.

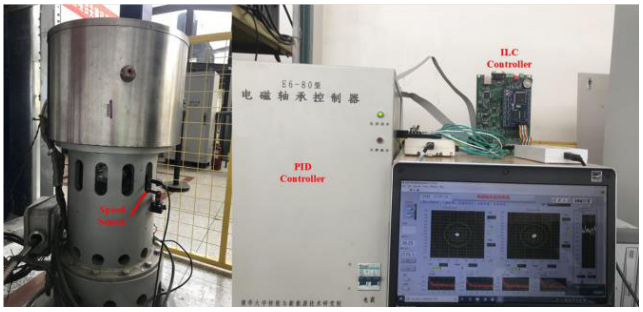

FIGURE 11. The AMB experimental system.

In addition, in the perspective of the rotor dynamics, the rotor spins around its inertia axis under this SCCM, and the periodic vibrations can be suppressed completely, which is suitable for the rotor unbalance control of AMB-RS in high-speed fields. And the SCCM final achieved in DCS is shown in Fig.9.

In Fig.7 and Fig.9, the filters are used to extract the control error as described in 3.1. Additionally, in equations (43) and (44), if the ILC input is set to zero, the system is reset to

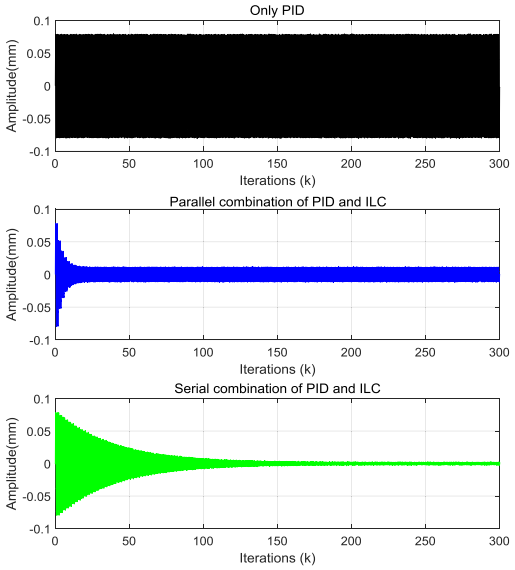

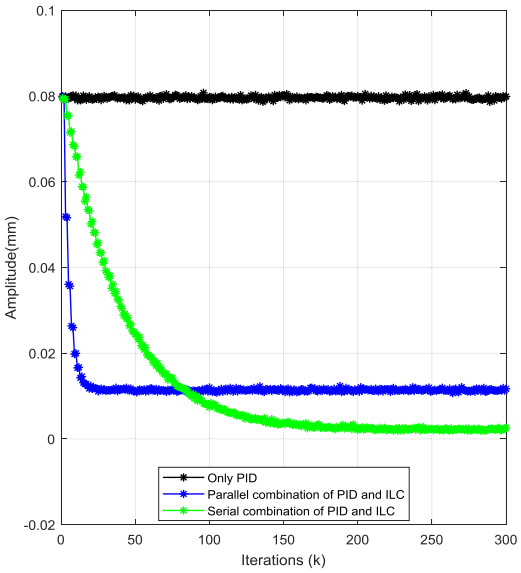

FIGURE 12. The results of simulations.

the original closed-loop feedback control mode. So it can be seen that this two compound control modes can easily achieve the plug-in control mechanism without changing the original CFCS. In other word, there is no need to redesign the FC in the practical application, which has greatly important application value in the unbalanced control of AMB-RS. For example, these methods can greatly reduce the implementation difficulties and redesign cost when they are used to optimize the performance of AMB-RS.

IV. EXPERIMENTAL RESEARCH

In order to verify the effectiveness of the control algorithm and control strategy, we carried out experimental researches on an AMB experimental system. Before that, numerical simulation was carried out with the parameters consistent with the AMB experimental system, to provide references for the experimental research.

A. INTRODUCTION TO THE AMB EXPERIMENTAL SYSTEM

Since the rotor is driven and controlled by a motor in the radial rotation, so a group of axial thrust bearings and two groups of radial bearings are usually required to achieve the active control in five DOFs. A vertical AMB structure is shown in Fig.10.

The AMB experimental system adopted in this paper is the vertical structure as shown in Fig.10, and the AMB experimental system is shown in Fig.11. Additionally, the control parameters of one DOF are shown in Table 1.

Here, the speed sensor in Fig.11 is used to detect rotor speed information, and the phase information of the speed is used to trigger each iteration of ILC. The AMB experimental system adopts a self-developed digital control system, the FC (PID) and ILC are all developed based on TMS320F28335. Meanwhile, control algorithms

TABLE 1. The control parameters of the AMB experiment system in one DOF.

Control parameter	Value
m	62kg
k_{xi}	145N/A
k_x	62500N/m
K_{PA}(including coefficient of DAC)	1.44×10^{-3}A
K_{DS}(including coefficient of ADC)	2.4×10^{7}/m
f_s	1×10^{4}Hz
k_p	20
τ_i	20s
τ_d	4×10^{-3}s

are developed on the Code Composer Studio 8.1.0 environment, and flash_debug mode is adopted to observe parameters. In addition, NI USB 6215 with the frequency of 10 kHz is used to acquire the displacement signal of each control channel for real-time monitoring.

Finally, experiments are conducted according to the ILC method described in equations (22), (36),(37) and (38) and the control strategies designed in Fig.7 and Fig.9. And k_{BC} expressed in equation (38) can be set to one ($k_{BC} = 1$) with the convergence criterion of the ILC algorithm and the system control parameters given in Table 1.

B. NUMERICAL SIMULATION RESEARCH

The parameters of the AMB experimental system shown in Table 1 are used for numerical simulation. Furthermore, a sine periodic disturbance is added in the control loop to simulate the periodic vibration produced by the balance force described in equation (12) and (13), and a random white noise is added in the control loop to simulate the non-periodic vibration caused by random interference.

Considering the rate of ILC proposed in this paper is slower, here $k = 300$ is set to better observe the control

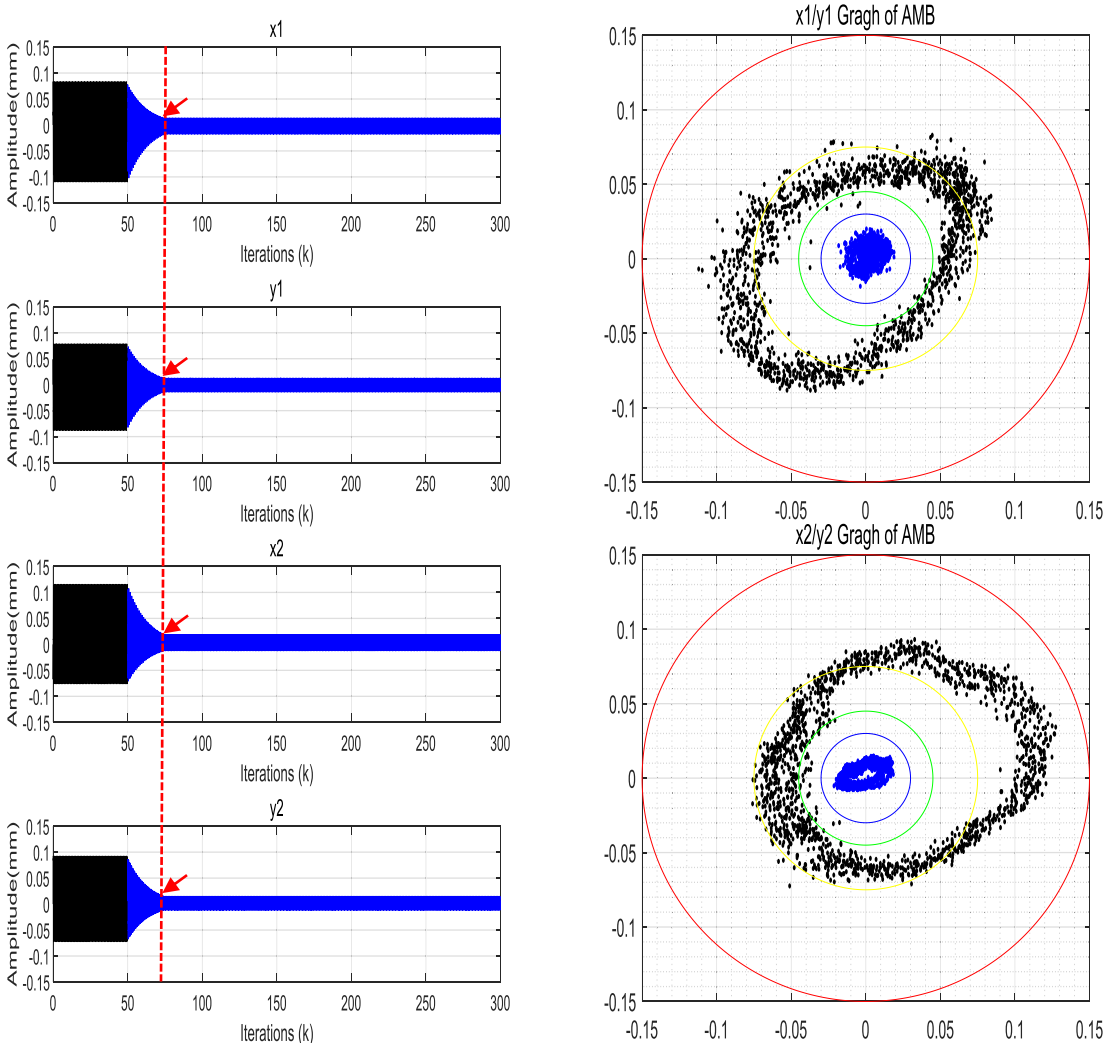

FIGURE 13. The experimental results of PCCM.

process. And we carried out three simulations, which are Only PID, PCCM (Parallel combination of PID and ILC) and SCCM (Serial combination of PID and ILC). Specially, the parameters of three simulations are completely consistent except for the inconsistent combination mode of controllers, and the results of simulations are shown in Fig.12.

In Fig.12, we can see that the disturbance cannot be gradually suppressed as the system is only controlled by PID under repetitive control, because PID algorithm cannot utilize the previous system information for self-learning. On the contrary, when the ILC loop is active, the periodic disturbance is obviously suppressed under repetitive control. Furthermore, the rate of disturbance suppression in PCCM is faster than in the SCCM, but the degree of disturbance suppression in SCCM is better than in PCCM, which are related to the control mechanism of the two compound control modes.

In PCCM, two controllers perform in parallel and generate control signals to suppress the disturbances simultaneously, so the rate of disturbance suppression is faster. However, there exists asynchronous characteristic as PID and ILC perform independently but interact with each other in the output of controllers, so some periodic disturbance is still left in the end. Instead, in SCCM, since the ILC adjusts the control errors independently, so the rate of disturbance suppression is slower. But there does not exist asynchronous characteristic as PID and ILC perform independently and without interacting with each other, so the final suppression effect on periodic disturbance is better.

C. EXPERIMENTAL RESEARCHE

In order to achieve the compound control modes designed above on the basis of the original AMB control system, the ILC and the hardware analog adder are designed and developed before the experimental research. Finally the AMB experimental system is upgraded and shown in Fig.11, and used to verify the control methods proposed above. As unbalanced force on the rotor only acts in four radial directions, so the displacement of four radial directions and the axis

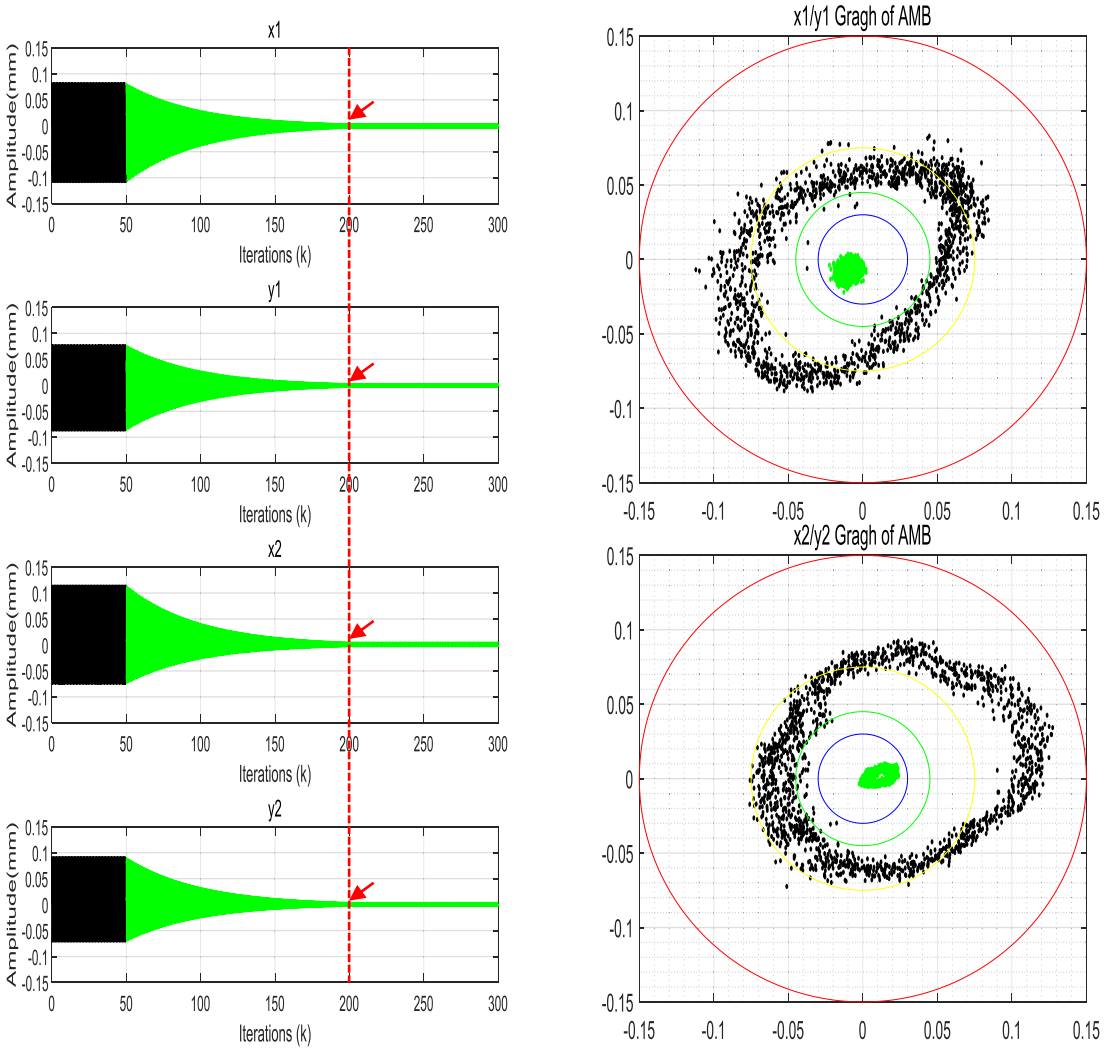

FIGURE 14. The experimental results of SCCM.

loci of the upper and lower ends are observed in real time, which serve as the basis for analyzing and evaluating the experimental results. Here, the experiments are carried out at the $f = 25$ Hz (the speed of rotor is 1500 r/m), because synchronous vibration is very serious as the AMB works in this frequency.

Similarly, the parameters of the two groups of experiment are completely consistent except for the inconsistent combination mode of controllers, and the results of experiments are shown in Fig.13 and Fig.14.

As we can see from the experimental results, firstly, the convergence rate shown in Fig.13 is faster than shown in Fig.14. In Fig.13, the system control error converges to a constant range at about the 15th ($k = 15$), but there are still some periodic vibration components (about left 25%). In Fig.14, it needs about the 150th ($k = 150$), and there are almost little periodic vibration components (about left 10%).

Secondary, in the perspective of the axis loci, in Fig.13, the ultimate vibration displacements of the rotor are constrained within the safest range and the rotor can spin around the geometric axis (coordinate origin (0,0)) well. That is to say, the center of axis loci of the rotor is the geometric axis under PCCM. Therefore, this control mode is more suitable for the unbalance control of AMB-RS in high-precision fields. In Fig.14, the ultimate vibration displacements of the rotor are bound in a very small range, but it is not symmetrical distribution around the geometric center, which means that the rotor spins around its inertia axis in the theory of rotor dynamics. That is to say, the vibration amplitude of the rotor can be well suppressed, but the axis loci of the rotor is uncertain. Therefore, this control method is more suitable for the unbalance control of AMB-RS in high-speed fields. Attentively, the inertia axis is not completely overlap with the geometric axis.

In conclusion, the results of simulation and experiment show that the two compound control modes have their own advantages and disadvantages.

V. CONCLUSION AND DISCUSSION

The unbalanced control is a key issue in the application of AMB and is one of the advantages of AMB than traditional mechanical bearing. From the research results, the ILC algorithm and control mechanisms proposed in this paper have a good control effect on the unbalance control of AMB-RS, and the main performances are listed as follows:

Firstly, in the process of signal filtering, repetitively calling system functions in the DSP embedded system would lead to the real-time performance of the control loop is difficult to ensure. The novel ILC algorithm proposed in this paper is helpful to achieve the parallel computation of three processing processes in the control system, and can ensure the real-time performance of the ILC loop, which is the basis of the application of the control method.

Secondary, the PCCM has certain asynchronous character, but it can improve the rate of control error. Contrary, the rate is slower under SCCM, but the control error can be compensated effectively. In other words, these two modes can achieve the different control objectives, provide the theoretical and technical basis for the unbalance control of AMB-RS in high-precision and high-speed fields.

Although the ILC method of unbalance control studied in this paper has achieved remarkable control effect, there are still lots of problems need to be tackled. After that, we will carry out researches and experiments in the following aspects: how to ensure the ILC requirements of unbalance control for AMB-RS in the case of abnormal data at the measuring side; how to achieve the effectiveness of ILC in the case of variable length as the rotational speed is changed, and so on. Summary, the principle of the method proposed is simple and is convenient to implement, if the related problems are solved, it has great engineering application value.

REFERENCES

[1] G. Schweitzer, and E. H. Maslen, *Magnetic Bearings: Theory, Design, and Application to Rotating Machinery*, Eds. Berlin, Germany: Springer, 2009.

[2] C. Di, I. Petrov, J.-J. Pyrhönen, and X. Bao, "Unbalanced magnetic pull compensation with active magnetic bearings in a 2 MW high-speed induction machine by FEM," *IEEE Trans. Magn.*, vol. 54, no. 8, Aug. 2018, Art. no. 8202913.

[3] G. Schweitzer. (1985). *Magnetic Bearings for Vibration Control*. [Online]. Available: http://community.ebooklibrary.org/

[4] K.-Y. Lum, V. T. Coppola, and D. S. Bernstein, "Adaptive autocentering control for an active magnetic bearing supporting a rotor with unknown mass imbalance," *IEEE Trans. Control Syst. Technol.*, vol. 4, no. 5, pp. 587–597, Sep. 1996.

[5] X. Xu, J. Fang, G. Liu, and H. Zhang, "Model development and harmonic current reduction in active magnetic bearing systems with rotor imbalance and sensor runout," *J. Vib. Control*, vol. 21, no. 13, pp. 2520–2535, Oct. 2015.

[6] C.-W. Lee, Y.-K. Yoon, and H.-S. Jeong, "Compensation of tool axis misalignment in active magnetic bearing spindle system," *KSME Int. J.*, vol. 11, no. 2, pp. 155–163, Mar. 1997.

[7] C. Peng, J. Sun, X. Song, and J. Fang, "Frequency-varying current harmonics for active magnetic bearing via multiple resonant controllers," *IEEE Trans. Ind. Electron.*, vol. 64, no. 1, pp. 517–526, Jan. 2017.

[8] K. Jiang and C. Zhu, "Multi-frequency periodic vibration suppressing in active magnetic bearing-rotor systems via response matching in frequency domain," *Mech. Syst. Signal Process.*, vol. 25, no. 4, pp. 1417–1429, Mar. 2011.

[9] K. Zhang and X.-Z. Zhang, "A review of unbalance control technology of active magnetic bearings," *China Mech. Eng.*, vol. 21, no. 8, pp. 897–903, Apr. 2010.

[10] Y. He, "Research on unbalance control for multi-variable active magnetic bearing system," Ph.D. dissertation, INET, Tsinghua Univ., Beijing, China, 2017.

[11] P.-C. Tung, M.-T. Tsai, K.-Y. Chen, Y.-H. Fan, and F.-C. Chou, "Design of model-based unbalance compensator with fuzzy gain tuning mechanism for an active magnetic bearing system," *Expert Syst. Appl.*, vol. 38, no. 10, pp. 12861–12868, Sep. 2011.

[12] S. Okubo, Y. Nakamura, and S. Wakui, "A design method of a mode control and an unbalance vibration control for five-axes active magnetic bearing systems," *Int. J. Adv. Mech. Syst.*, vol. 5, no. 4, pp. 257–269, 2013.

[13] C. Bi, D. Wu, Q. Jiang, and Z. Liu, "Automatic learning control for unbalance compensation in active magnetic bearings," *IEEE Trans. Magn.*, vol. 41, no. 7, pp. 2270–2280, Jul. 2005.

[14] Y. Liu, S. Ming, S. Zhao, J. Han, and Y. Ma, "Research on automatic balance control of active magnetic bearing-rigid rotor system," *Shock Vib.*, vol. 2019, Jan. 2019, Art. no. 3094215.

[15] C. Kang and T.-C. Tsao, "Control of magnetic bearings for rotor unbalance with plug-in time-varying resonators," *J. Dyn. Syst., Meas., control*, vol. 138, no. 1, Oct. 2015, Art. no. 010111.

[16] Z.-Z. Tang, Y.-J. Yu, Z.-H. Li, and Z.-T. Ding, "Disturbance rejection via iterative learning control with a disturbance observer for active magnetic bearing systems," *Frontiers Inf. Technol. Electron. Eng.*, vol. 20, no. 1, pp. 131–140, Jan. 2019.

[17] J.-X. Xu, S.-K. Panda, and T.-H. Lee, *Real-time Iterative Learning Control: Design and Applications*. London, U.K.: Springer, 2009.

[18] D. Shen, *Iterative Learning Control with Passive Incomplete Information: Algorithms Design and Convergence Analysis*. London, U.K.: Springer, 2018.

[19] D. Shen and J.-X. Xu, "A novel Markov chain based ILC analysis for linear stochastic systems under general data dropouts environments," *IEEE Trans. Autom. Control*, vol. 62, no. 11, pp. 5850–5857, Nov. 2017.

[20] J.-X. Xu and Y. Tan, *Linear and Nonlinear Iterative Learning Control*. New York, NY, USA: Springer, 2003. [Online]. Available: https://link.springer.com/

[21] D.-H. Owens, *Iterative Learning Control*. London, U.K.: Springer, 2016. [Online]. Available: https://link.springer.com/

[22] D. Shen and Y. Wang, "ILC for networked nonlinear systems with unknown control direction through random lossy channel," *Syst. Control Lett.*, vol. 77, pp. 30–39, Mar. 2015.

[23] D. Shen, W. Zhang, Y. Wang, and C.-J. Chien, "On almost sure and mean square convergence of P-type ILC under randomly varying iteration lengths," *Automatica*, vol. 63, pp. 359–365, Jan. 2016.

[24] Y. Wang, Y. Yang, and Z. Zhao, "Robust stability analysis for an enhanced ILC-based PI controller," *J. Process Control*, vol. 23, no. 2, pp. 201–214, Feb. 2013.

[25] Y. Wang, H. Zhang, S. Wei, D. Zhou, and B. Huang, "Control performance assessment for ILC-controlled batch processes in a 2-D system framework," *IEEE Trans. Syst., Man, Cybern., Syst.*, vol. 48, no. 9, pp. 1493–1504, Sep. 2018.

[26] X.-S. Dai, X.-Y. Zhou, S.-P. Tian, and H.-T. Ye, "Iterative learning control for MIMO singular distributed parameter systems," *IEEE Access*, vol. 5, pp. 24094–24104, 2017.

[27] Q. Yan, J. Cai, L. Wu, and Q. Zhou, "Error-tracking iterative learning control for nonlinearly parametric time-delay systems with initial state errors," *IEEE Access*, vol. 6, pp. 12167–12174, 2018.

[28] Y. Zheng, X. Liu, G. Yang, H. Zuo, Z. Sun, and Z. Shi, "Analysis and experimental study on uncertain fault of active magnetic bearing displacement sensor," *Appl. Comput. Electromagn. Soc. J.*, vol. 34, no. 4, pp. 619–624, Apr. 2019.

[29] I. S. Kuseyri, "Robust control and unbalance compensation of rotor/active magnetic bearing systems," *J. Vib. Control*, vol. 18, no. 6, pp. 817–832, May 2012.

[30] Y. Zheng, N. Mo, Y. Zhou, and Z. Shi, "A model-free control method for synchronous vibration of active magnetic bearing rotor system," *IEEE Access*, vol. 7, pp. 79254–79267, 2019.

[31] O. Robert, *DSP Software Development Techniques for Embedded and Real-Time Systems*. Amsterdam, The Netherlands: Elsevier, 2006.

[32] D.-A. Bristow, "Iterative learning control for precision motion control of microscale and nanoscale tracking systems," Ph.D. dissertation, Dept. Mech. Eng. Graduate College, Univ. Illinois Urbana-Champaign, Champaign, IL, USA, May 2007.

[33] R. W. Longman, "Iterative learning control and repetitive control for engineering practice," *Int. J. Control*, vol. 73, no. 10, pp. 930–954, 2000.
[34] D. De Roover and O. H. Bosgra, "Synthesis of robust multivariable iterative learning controllers with application to a wafer stage motion system," *Int. J. Control*, vol. 73, no. 10, pp. 968–979, 2000.
[35] R. Longman, "Designing iterative learning and repetitive controllers," in *Iterative Learning Control*, Eds., Z. Bien, and J.-X. Xu, Norwell, MA, USA: Kluwer, 1998.

YANGBO ZHENG received the B.S. degree from the Department of Automation, North China Electric Power University (NCEPU), China, in 2007, and the M.S. degree from the Shenyang Institute of Automation (SIA), Chinese Academy of Sciences (CAS), China, in 2010. He is currently pursuing the Ph.D. degree with the Institute of Nuclear and New Energy Technology (INET), Tsinghua University, China. His research interest includes active magnetic bearing control technology.

NI MO was born in Hunan, China, in 1982. He received the M.S. and Ph.D. degrees in electrical engineering (EEA), Tsinghua University, China, in 2004 and 2009, respectively, where he is currently an Associate Researcher with the Institute of Nuclear and New Energy Technology (INET). His research interests include control applications and electrical designing in optimization of magnetic bearing systems.

YAN ZHOU received the B.S. and M.S. degrees from the Department of Automation, Beihang University, China, in 2002 and 2005, respectively. She is currently with the Institute of Nuclear and New Energy Technology (INET), Tsinghua University. Her research interests include active magnetic bearing (AMB) amplifiers and control systems and its applications.

ZHENGANG SHI received the B.S. degree in engineering physics from Tsinghua University, China, in 1997, and the M.S. and Ph.D. degrees from the Institute of Nuclear and New Energy Technology (INET), Tsinghua University, in 2000 and 2003, respectively, where he is currently the Head of the Magnetic Bearing Laboratory. His research interests include magnetic bearing technology and nuclear power generation technology.